Using Electric Field to Monitor the Continuous Casting

R. S. Qin[1]

[1]School of Engineering and Innovation, The Open University, Walton Hall, Milton Keynes WA76AA, United Kingdom

Abstract— Detecting the internal dynamic structure in opaque production line helps to obtain essential information for steering the processing parameter. This work reports the implementation of electric field and magnified percolation effect to a continuous casting mold. It is able to indicate the change of internal dynamic structure such as the solid shell thickness, nozzle condensation, structural integrity of coating film, slag entrapping and inclusion states. The method does not suffer from the penetration limit from skin effect of electromagnetic field and has potential to detect the structural health of engineering component made by multiphase alloys.

1. INTRODUCTION

Characterization of internal structure in bulk metallic materials has been challengeable due to the penetration limit of acoustic and electromagnetic waves in metals [1]. Other detection methods, e.g. neutron diffraction and tomography, are not suitable to the engineering production site. Electric current percolation as a well-known phenomenon in multiphase conductive materials [2], however, can work without the restriction to penetrate through the bulk volume. Current tends to flow along the highest conductive path, and the conductivity is sensitive to the structure of bulk phase [3] and interface [4]. Measurement of percolation has been implemented to characterize the cracking of nanomaterials [5] and structural health of composites [6]. For many other cases, however, percolation is either too weak to be measurable or indicates ambiguous structural possibilities [7]. The motivation of this work is to magnify the weak percolation to significant level and to apply the configuration to screen and steer the continuous casting processing.

Continuous casting provides over 90% of annual global steel production and significant amount of aluminium, magnesium and copper manufacturing. The cast mold in steel processing is made by copper with embedded cooling devices, coated with crystalline and glassy slag films in its internal surface, containing solid mold powder, liquid mold flux, solidified metal shell, nozzle and liquid metal [8][9], as is demonstrated schematically in Fig.1. The dimension and properties of the structure affect the heat transfer, phase transition, casting rate, cast quality and manufacturing safety. The thickness of solidified metal shell is affected by horizontal heat transfer and casting rate, with too thick to affect productivity and too thin to cause safety issue. The clogging of nozzle is caused by the condensation of oxide inclusions to the nozzle bore surface and affects the processing continuity. The failure of structural integrity in coated slag film damages lubrication and surface quality. The inclusions and entrapping of slags degrade the products. Monitoring the internal dynamic structure during production is desirable for the engineering manufacturing.

Measurement of electric current requires to arrange a pair of electrodes in adequate positions. The positive electrode (anode) is located inside the nozzle. This can maximize the percolation and make the working status of the nozzle detectable. In practical engineering, this is achievable because the anode can be submerged into the liquid metal in turdish to produce the same effect as that in the nozzle. The negative electrode (cathode) is to attach to the surface of various positions according to different purposes. For examples, to detect the thickness of solidified metal shell and the nozzle condensation the cathode is arranged to touch the outside surface of the cast using a conductive fibre brush, as that indicated in Fig. 1. To monitor the structural integrity of the coated slag film the cathode should be attached to the outside surface of the copper mold. When a constant electric potential difference is applied to the electrodes, the current flows from anode to the cathode without leaking. The percolation path affects the effective electrical resistance and hence the current.

2. COMPUTATIONAL METHODS

To calculate the electric current distribution in the mold, the system is discretised into lattice and time is discretised into successive steps. The relaxation method is used to calculate the static

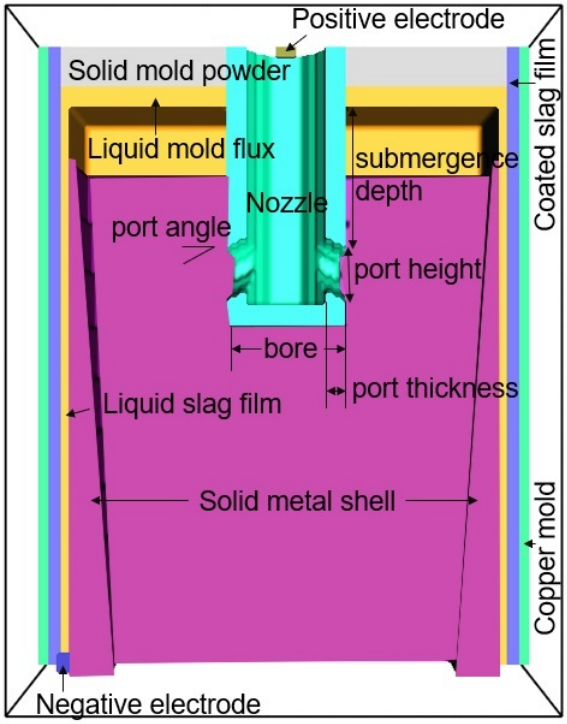

Figure 1: Schematic plotting of continuous casting mold and electrodes.

distribution [10]. For uniform rectangular lattice, each grid apart from that on the surface has 6 nearest neighbouring sites in the same distance. The time iteration during relaxation in adiathermal approximation is obtained by Kirchhoff's circuit law as

$$\psi_j^{t+1} = \frac{\sum_{i=0}^{6} \psi_i^t \sigma_{ij}}{\sum_{i=0}^{6} \sigma_{ij}} \tag{1}$$

where ψ_i^t is the electrical potential at position i at time step t. σ_{ij} is the electrical conductivity between sites i and one of its nearest neighbours j. In the case when i and j are located in two different phases, it is assumed that the interface is in perpendicular bisector of the line between i and j, and the interface makes no extra contribution to the electrical resistance between two sites due to its negligible thickness and limit value [11]. The electrical conductivity between two next sites can be expressed generally as

$$\sigma_{ij} = \frac{2\sigma_i \cdot \sigma_j}{\sigma_i + \sigma_j} \tag{2}$$

When the static electrical potential distribution has been obtained, the electric current between two neighbouring sites is obtainable by Ohm's law.

$$I_{ij}^t = \Delta l \cdot \sigma_{ij}(\psi_i^t - \psi_j^t) \tag{3}$$

where Δl is the lattice distance. The computational method can be easily manipulated to irregular or adaptive lattices, where the number of the nearest neighbours might not be 6 and the conductivity should be replaced with conductance to include the geometric dimensions of the lattice. For the uniform rectangular lattice, the curved surface is approximated by staircases. The relaxation iteration is considered to achieve a static state when the change of electric potential at all the grids is smaller than a critical value (δ).

$$\sum_i |\psi_i^{t+1} - \psi_i^t| < \delta \tag{4}$$

The summation goes throughout the whole volume of the computing system. The smaller critical value requires longer computing time but more accurate results.

There are two types of boundaries. The first is for the electrodes. The electrical potential takes a fixed value that has been defined in anode or cathode. The second is for those sites on the surface apart from electrodes, where the electric current in perpendicular to the surface is vanished. The numerical calculations are performed to a system with the dimension and parameters listed in Table 1. The thickness of copper mold is significant thinner than the reality but does not affect the results due to highest conductivity in the system. The rest of the dimensions are defined after reference to the reality. The port angle is defined as $\pi/6$. The terminology is indicated in Fig. 1. The metal starts to solidify below the liquid mold flux from the cooled copper mold wall. The thickness of the solid shell is approximated as [15].

$$d = c\sqrt{h} \tag{5}$$

where d is the thickness and h the distance from the top of the solid shell. c is a coefficient dependent on the heat transfer and is called the solid shell coefficient. The positive electrode is connected to 20 volts electric potential. The negative electrode is given 0 volts of electric potential.

Parameter		Dimension (m)	Electrical conductivity ($\times 10^6 S/m$)
Copper mold			5.56 (at 1100 K)
	width	0.241	
	height	0.300	
	depth	0.121	
	thickness	0.006	
Nozzle			3.52×10^{-9} (at 1700 K) [12]
	bore	0.060	
	port thickness	0.010	
	port height	0.026	
	submergence depth	0.100	
Thickness			
	solid mold power	0.020	10^{-7}
	liquid mold flux	0.010	10^{-4} [13]
	liquid slag film	0.004	10^{-4} [13]
	coated slag film	0.006	5.0×10^{-6}
Electrode			
	height	0.006	5.56
	radius	0.006	5.56
Liquid steel			0.659 [14]
Solid steel			0.842 [14]

3. NUMERICAL RESULTS AND DISCUSSION

Using $\Delta l = 0.002m$ and initial condition of the electric potential to be distributed with the same gradient from top to bottom of the system, the electric potential and electric current after 360,000 relaxation time-steps for $c = 0.2$ is plotted in Fig.2. Fig. 2(a) shows the contour distribution of electric potential in $z = 0.06m$ cross section. The asymmetric distribution of electric potential in Fig. 2(a) is caused by the asymmetric arrangement of cathode. The electric distribution at this section is demonstrated in Fig. 2(b). The largest current flowing through two adjacent grids in the system is $2.282 \times 10^{-3}A$, which is equivalent to a current density of $570.5A/m^2$ and is located at a corner at the surface of both electrodes. The current density inside the nozzle and port is higher than that outside the nozzle, as is shown in Fig. 2(b). To demonstrate the percolation effect, Fig. 2(c) and 2(d) shown the current distribution in smaller current scale. Fig. 2(c) shows clearly the percolation. Electric current chooses not only the shortest possible path from anode to cathode but also the path with highest conductivity. The latter is denoted in a label A in solidified metal shell which has higher conductivity than that in liquid metal. Fig. 2(d) shows symmetric distribution of current and percolation flow in the solidified metal shell. The current amplitude 1.2A corresponds to a current density $3A/m^2$, which is very low.

To show the magnified percolation, the electrical resistance of the liquid and solidified metal mixtures can be calculated using the given dimension. This is found around 13.42 Ω for 100% solid and 17.15 for 100 % liquid. The difference is 3.73 Ω only. When the shell coefficient (c) is changed from 0.15 to 0.2, the volume fraction of solidified metal shell changes from 26.8% to 37.96%. Using the volume fraction approximation [16], the electrical resistance changes from 16.15 Ω to 15.73 Ω,

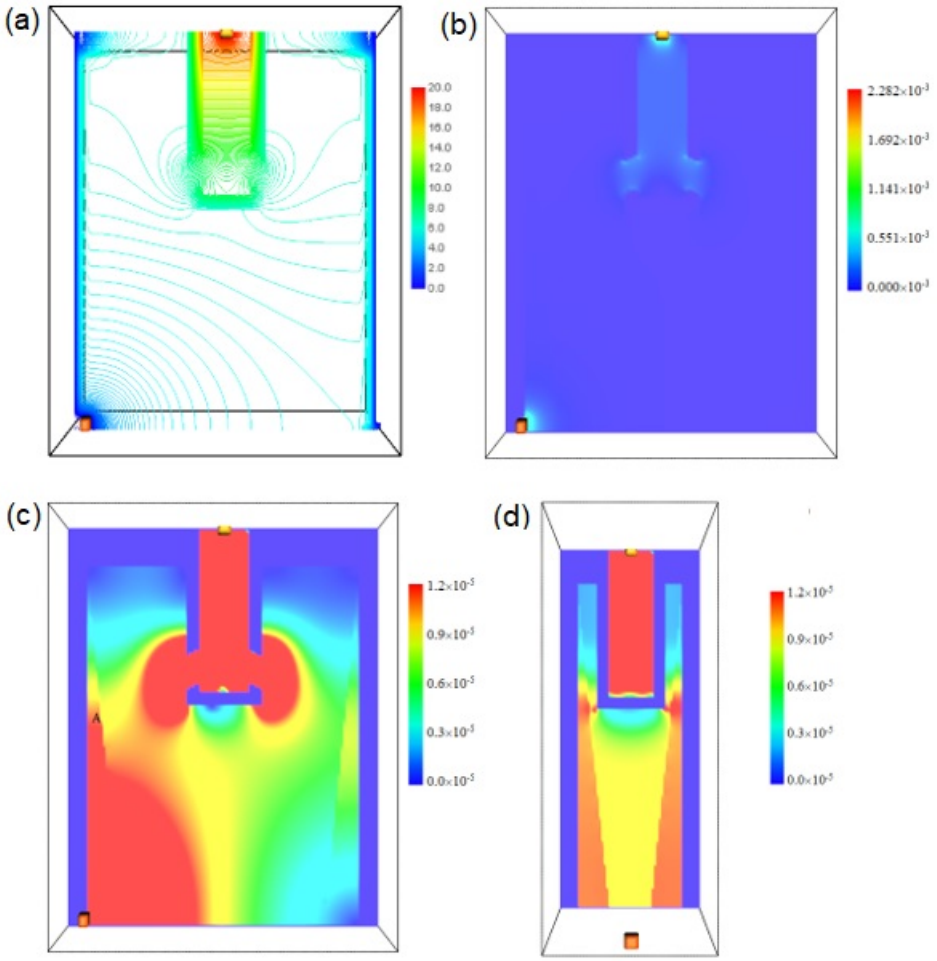

Figure 2: The distribution (c=0.2) of (a) electric potential and (b) electric current at $z = 0.06m$; rescaled current distribution at (c) $z = 0.06m$ and (d) $x = 0.12m$, respectively.

which is a reduction of 0.42 Ω only. To examine that in the device of present work, the total electric current and the effective electrical resistance has been calculated. The current was calculated in a cross section at $0.1m$ above the bottom line. The effective electrical resistance was calculated by the Ohm's law. The results are presented in Fig. 3(a) and 3(b). It is found that the resistance from $c = 0.15$ to 0.2 is reduced by 2.82 Ω, which is 6 times larger than the estimation. The overall change of electrical resistance from $c = 0.15$ to 0.45 is 9.73 Ω, which is more than 2.6 times of the possible range of 3.73 Ω. The percolation effect is magnified significantly.

It is important to discuss why the overall effective electrical resistance in the current device is significantly larger than the estimated value in the same volume and shape of solid and liquid metal. This is due to two major reasons: a) the refractory nozzle which confined the current in a narrow space; and b) the effective conductive cross area in the liquid metal below the nozzle is reduced substantially, as is shown in Fig. 2. The shape of the nozzle and the arrangement of electrodes magnifies percolation.

Liquid metal contains non-metallic oxides. These might be inherited from the earlier stage processing or formed continuously in the cast mold via chemical reaction. The oxide inclusions can condense to the inner surface of nozzle and cause port height to reduce until to be blocked completely [17]. The phenomenon is called nozzle clogging and can affect a wide variety of spraying processing. Electromagnetic stirring and high frequency electric pulses have been implemented to reduce the clogging [18][19]. The method to be discussed here is to identify the stage to implement clogging treatments.

The non-metallic oxides have smaller conductivity than that of the liquid steel [20]. The flowing electric current is being reduced during the condensation of oxide layer in the inner surface of nozzle. Measurement of the electric parameters in the cast mold using the device demonstrated in Fig.1

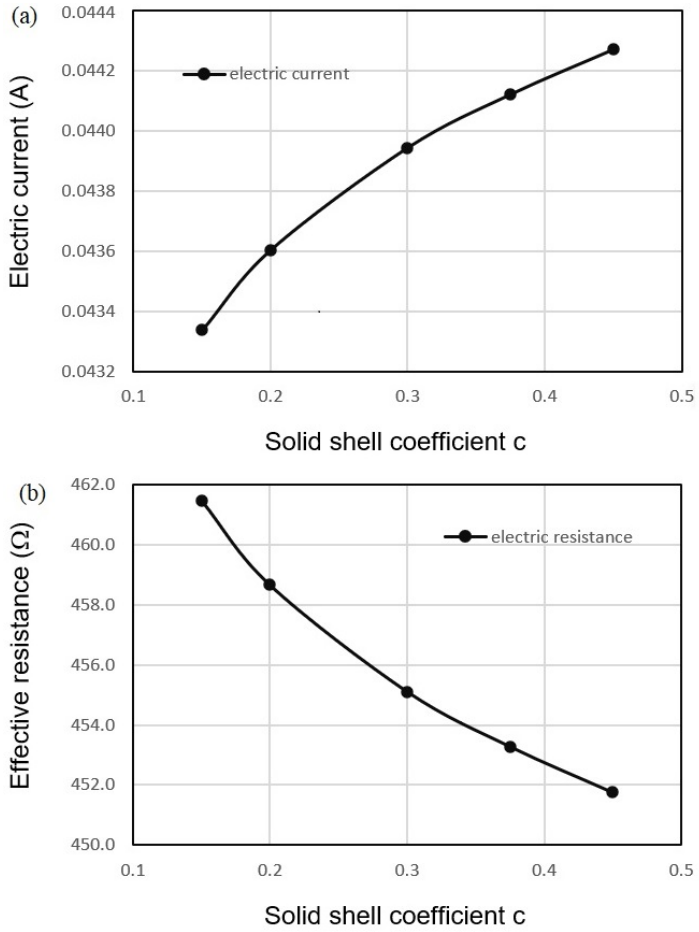

Figure 3: (a) Numerical results for electric current vs. solid shell coefficient; (b) effective electrical resistance vs. solid shell coefficient.

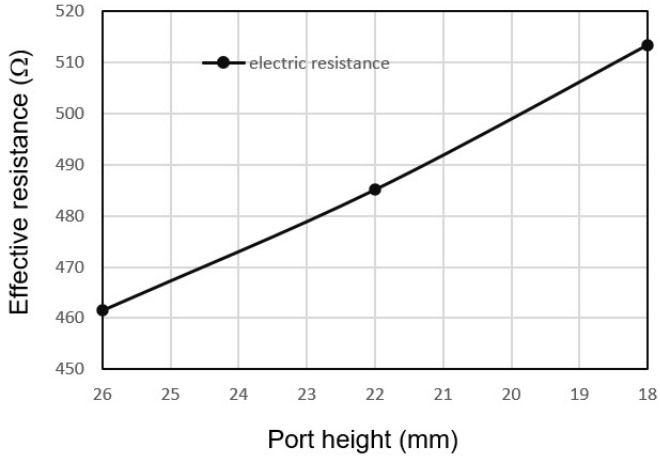

Figure 4: (a) The numerical results for the change of effective electric resistances as the port height is reduced from $0.026m$ to $0.018m$ due to oxide condensation.

can detect the thickness of the condensation layer. Fig.4 illustrates the numerical results when the port height of the nozzle is reduced from $0.026m$ to $0.022m$ and then to $0.018m$ due to oxide condensation. The reducing port height increases the effective electrical resistance of the system sensitively, as is shown in Fig.4. The port plays a role of bottleneck to the current flow. Electric current will not be able to flow through the part when it is clogged completely. The continuous casting will be disrupted in that case. The method in this work can predict the stage to turn on anti-clogging treatment.

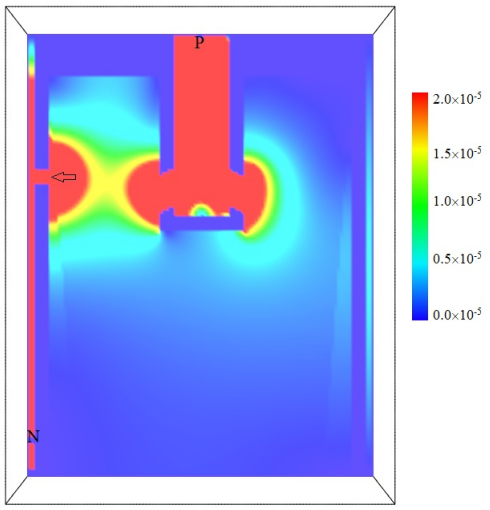

Figure 5: (a) Detection of the coating film integrity, where P, N and arrow denote the location of anode, cathode and a crack, respectively.

Following the same principle, the effective electrical resistance increases if the volume fraction of oxide inclusions increases. The latter is mainly caused by the slag and mold flux entrapping due to the improper control of fluid flow in liquid metal. However, the increasing behaviour of the effective electrical resistance in slag entrapping is different from that in nozzle clogging. The former has the persistent changing, but the latter is in fluctuation because the entrapped slag is pulled down with the cast. Our previous research has demonstrated that the electric current can push the inclusion out of the liquid metal [20] and prevent the agglomeration of inclusions[21]. However, the effect is proportional to the square of electric current density[10][22]. High density electric current can also affect the microstructure in solid metal [23]. However, the current density implemented in the present work is a few orders of magnitudes smaller than that in other experiments [20][21][22] and is also lower than the critical value to induce change in solid materials[24].

The coated solid slag film usually contains crystalline and glassy layers[8]. Their electrical conductivities are as low as 10^{-5} to 10^{-6} S/m. For a thin film with thickness around $0.006m$ and cross section of $0.300m \times 0.121m$ the electrical resistance is over 10^4 Ω. This is about two orders of magnitude greater than that of the effective resistance showing in Fig.3(b). Arranging the cathode to attach to the outside surface of copper cast is able to monitor the structural integrity of the coating slag film. Once it fails and form significant cracks, the liquid slag can get into the cracks of the coated layer. The effective resistance will drop significantly. Fig.5 demonstrates one of such cases, where P represents the location of anode and N represents the cathode position. The arrow points to a breakage where the current can go through.

In engineering practise, the cast mold will be replaced with new coating when the structural integrity of previous coating is failed. It is, therefore, unnecessarily to locate the failure position. However, it is possible to detect the failure position using the electric method. This is because the different failure positions with cause different value of the electrical resistance. Moving the negative electrode to several positions will be able to determine the failure position.

4. CONCLUSION

In summary, we have developed a method to detect the structural health of opaque internal structure in continuous casting mold using magnified current percolation, and has examined the cases to sense the change of solid shell thickness, condensation of oxide in the pore of nozzle, mold flux entrapping and cracking of coated slag layer. In the production lines, the most important issue is to monitor the change of the internal structure and understand the indication of the change rather than to reveal the details of the structure. The method developed in the present work is sufficient to monitor the changes and can be implemented in production line. A reduction of effective electrical resistance implies the growth of the solid metal shell. A substantial increase of the resistance indicates the developing clogging. A sudden fluctuation of the resistance indicates the improper fluid flow behaviour that has caused the entrapping of mold flux. The online data obtained by the method can be feedbacked to the control room to adjust the processing condition and to optimize

the parameters. Moreover, the method developed in the present work can be used to monitor the structural health of the engineering component made by multiphase alloys. This is to measure the effective resistance of component in multiple pairs points and store the pattern as reference. The component after a certain stage of service can be measured again. The obtained new pattern is compared with the reference pattern to assess the changes. Any internal change of microstructure, e.g. formation of cracks and defects, alters the percolation and is measurable.

ACKNOWLEDGMENT

The work was sponsored by European Commission RFCS (No. 847269). The author is grateful to Dr. Bridget Stewart at Materials Processing Institutes and Dr. Ashutosh Bhagurkar at the Open University for fruitful discussions and to Drs. Karin Hansson-Antonsson and Fredrik A Axelsson at Sandvik in Sweden for provision of the mold powders for characterizing the electrical properties. The three-dimensional visual analysis of the computational data was generated using MatVisual software.

REFERENCES

1. Shen, C., Xu, J., Fang, N. X. and Jing, Y., "Anisotropic complementary acoustic metamaterial for canceling out aberrating layers," *Phys. Rev. X*, Vol. 4, No. 4, 041033, 2014.
2. Lux, F., "Models proposed to explain the electrical-conductivity of mixtures made of conductive and insulating materials," *J. Mater. Sci.*,Vol. 28, No. 2, 285–301, 1993.
3. Bohnenkamp, U., Sandstrom, R., and Grimvall, G., "Electrical resistivity of steels and face-centered-cubic iron," *J. Appl. Phys.*, Vol. 92, No. 8, 4402-4407, 2002.
4. Lu, L., Shen, Y. F., Chen, X. H., Qian, L. H. and Lu, K, "Ultrahigh strength and high electrical conductivity in copper," *Science*, Vol. 304, No. 5669, 422-426, 2004.
5. Liu, C. G., Ainsworth, C. A., Sampson, W. W. and Derby, B., "Fatigue and the electrical resistance of silver nanowire networks," *Scr. Mater.*, Vol. 181, 97-100, 2020.
6. Hu, C., Li, Z. Y., Wang, Y. L.,Gao, J. C., Dai, K., Zheng, G. Q., Liu, C. T., Shen, C. Y., Song, H. X. and Guo, Z. H., "Comparative assessment of the strain-sensing behaviors of polylactic acid nanocomposites: reduced graphene oxide or carbon nanotubes," *J. Mater. Chem. C*, Vol. 5, No. 9, 2318-2328, 2017.
7. Dong, W., Huang, Y. M., Lehane, B. and Ma, G. W., "XGBoost algorithm-based prediction of concrete electrical resistivity for structural health monitoring," *Automat. Constr.* Vol. 114, 103155, 2020.
8. Mills, K. C. andFox, A. B., "The role of mould fluxes in continuous casting—so simple yet so complex," *ISIJ Int.* Vol. 43, No. 10, 1479–1486, 2003.
9. Thomas, B. G. and Zhang, L. F., "Mathematical modeling of fluid flow in continuous casting," *ISIJ Int.* Vol. 41, No. 10, 1181–1193, 2001.
10. Qin, R. S. and Bhowmik, A, "Computational thermodynamics in electric current metallurgy," *Mater. Sci. Technol*, Vol. 31, No. 10, 1560–1563, 2015.
11. Qin, R. S. "Suppression of the surface roughness and fluctuation frequency by electric method," *Mater. Today Commun.*, Vol. 28, 102512, 2021.
12. Kwon, O. H., Jang, C. H., Lee, J. H., Jeong, H. Y., Kwon, Y. I., Joo, J. H. and Kim, H. J., "Investigation of the electrical conductivity of sintered monoclinic zirconia (ZrO_2)," *Ceram. Int.*, Vol. 43, No. 11, 8236-8245, 2017.
13. Haraguchi, Y., Nakamoto, M., Suzuki, M., Fuji-Ta, K. and Tanaka, T., "Electrical conductivity calculation of molten multicomponent slag by neural network analysis," *ISIJ Inter.* Vol. 58, No. 6, 1007-1012, 2018.
14. Ho, C. Y. and Chu, T. K., "Electrical resistivity and thermal conductivity of nine selected AISI stainless steels," report from American Iron and Steel Institute.
15. Meng, Y. A. and Thomas, B. G. "Heat-transfer and solidification model of continuous slab casting: CON1D," *Metall. Mater. Trans. B*, Vol. 34, 685-705, 2003.
16. Bohnenkamp, U. and Sandströma, R., "Electrical resistivity of steels and face-centered-cubic iron," *J. App. Phys.* Vol. 92, No. 8, 4402-4407, 2002.
17. Bai, H. and Thomas, B. G., "Effects of clogging, argon injection, and continuous casting conditions on flow and air aspiration in submerged entry nozzles," *Metall. Mater. Trans. B*, Vol. 32, No. 4, 707-722, 2001.

18. Li, B., Lu, H. B., Shen, Z. Sun, X. H., Zhong, Y. B., Ren, Z. M. and Lei, Z. S., "Physical modeling of asymmetrical flow in slab continuous casting mold due to submerged entry nozzle clogging with the effect of electromagnetic stirring," *ISIJ Inter.* Vol. 59, No. 12, 2264-2271, 2019.
19. C. Tian, J.K. Yu, E.D. Jin, T.P. Wen, D.B. Jia, L. Yuan, "Effect of interfacial reaction behavior on the submerged entry nozzle by the electric current pulse," *J. Alloys Comp.*, Vol. 809, 151825, 2019.
20. Zhang, X. F., W.J. Lu, Qin, R. S., "Removal of MnS inclusions in molten steel using electropulsing," *Scr. Mater.*, Vol. 69, 453-456, 2013.
21. Zhao, Z. C. and Qin, R. S., "Morphology and orientation selection of non-metallic inclusions in electrified molten," *Mater. Metall. Trans. B*, Vol. 48, No. 5, 2781-2787, 2017.
22. Zhang, X. F. and Qin, R. S., "Electric current-driven migration of electrically neutral particles in liquids," *Appl. Phys. Lett.*, Vol. 104, 114106, 2014.
23. Rahnama, A. and Qin, R. S. "Electropulse-induced microstructural evolution in a ferritic–pearlitic 0.14% C steel," *Scr. Mater.*, Vol. 96, 17-20, 2015.
24. Conrad, H., "Influence of an electric or magnetic field on the liquid–solid transformation in materials and on the microstructure of the solid," *Mater. Sci. Eng. A*, Vol. 287, 205–212, 2000.